**FIGURE S1.** Calibration lines for H$_2$O concentrations in olivine (light green) and orthopyroxene (dark green) by the Carnegie Cameca NanoSIMS 50L in August 2016. The X-axis is the measured $^{16}O^1H/^{30}Si$ ion ratio multiplied by the wt% SiO$_2$ concentration of each standard; the Y-axis shows the accepted H$_2$O concentration for each standard (concentrations and references given in Table 1). Symbol shape distinguishes published H$_2$O concentrations by method of analysis. The green shaded regions contain the regression and 95% confidence interval for the olivine and orthopyroxene standards. The calibration lines were fit using a weighted orthogonal-distance-regression (WODR) to account for uncertainty in both the measured element ratios and the known concentrations. Error bars represent 1 sigma uncertainties. Uncertainties in $^{16}O^1H/^{30}Si$ ion ratio * SiO$_2$ are smaller than the symbols. Uncertainty in the calibration was assessed with multiple regressions on bootstrapped samples consisting of 5000 random subsamples drawn with replacement from the measurements (Efron, 1979). Confidence intervals were determined from the histograms of possible H$_2$O concentrations in the bootstrapped calibration lines. Uncertainties for India Enstatite and ROM273 (15 and 29 ppm respectively) used in this calibration differ from published values (7 and 15 ppm) because we propagated errors from the FTIR calibration, which is solely dependent on KBH-1. All calibration lines have been fit to include Suprasil glass as a near-blank. Refer to Table 2 for slope, intercept and R2. The variability in the India Enstatite orthopyroxene is consistent with the presence of amphibole lamellae, as described by Mosenfelder and Rossman (2013a).
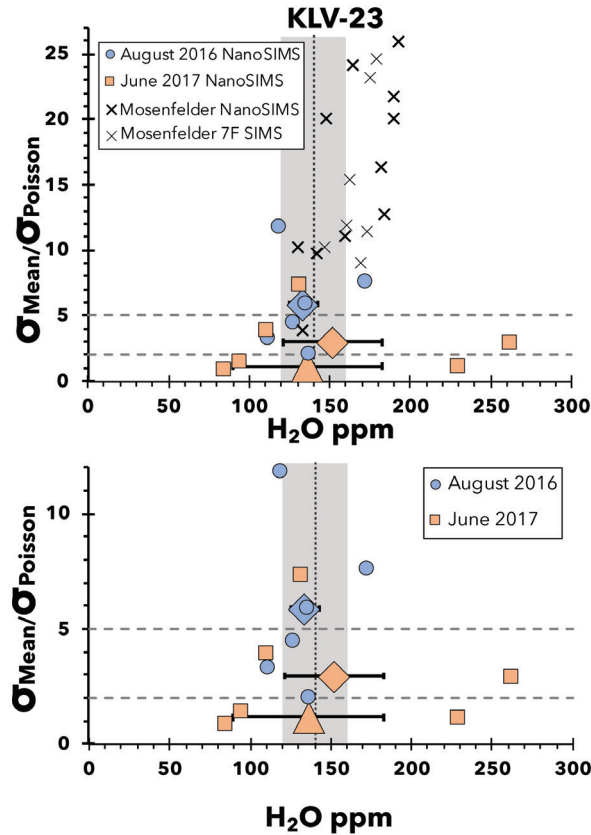
Figure S2. H$_2$O ppm in olivine KLV-23 calculated with the Bell03 calibrations for August 2016 (blue) and June 2017 (orange) nano-SIMS sessions at Carnegie, compared to published data (x symbols) from Mosenfelder et al. (2011). Diamonds represent the average of all concentrations in the two Carnegie sessions, while the triangle is the average of concentrations which meet the criterion of a $\frac{\sigma_{mean}}{\sigma_{Poisson}} > 2$, the ratio of the measured standard error (σ_{mean}) to the expected standard deviation for a number of total counts collected ($\sigma_{Poisson}$). The vertical dashed line and gray bar highlight the concentration Bell03 measured by NRA for KLV-23 (140 ±20 ppm). Lower panel is the same as upper, but with an expanded scale. The variability in this sample is due to the presence of hydrous, non-olivine inclusions (Mosenfelder et al., 2011), and it persists even for analyses with low $\frac{\sigma_{mean}}{\sigma_{Poisson}}$ (as in the June 2017 data). This demonstrates that filtering SIMS measurements by $\frac{\sigma_{mean}}{\sigma_{Poisson}}$ does not necessarily ensure all outliers from sample heterogeneity will be removed or that the mean of the accepted measurements will have a lower standard error than the whole population.
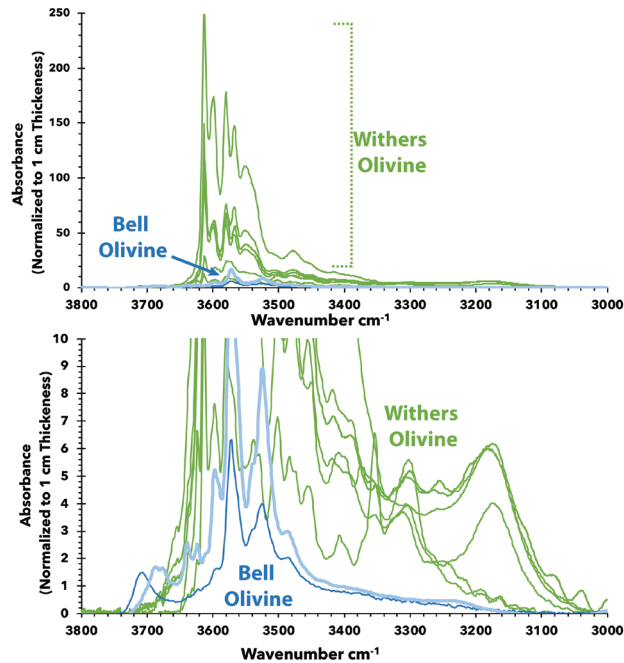
FIGURE S3. Plots of FTIR spectra for olivine from Bell03 and Withers12. Each spectrum is the sum of the three polarized spectra measured along each crystallographic axis for each sample. Blue spectra are from Bell03 olivine (KLV-23 [dark blue] and GRR1012 [light blue]). Green spectra are from all the olivines in Withers12. Plots in the lower panel have been magnified to show distinct peaks at lower wavenumbers (<3500 cm⁻¹) in the Withers12 spectra that are often overlooked unless the full range of absorbances are plotted. For a more detailed analysis of the specific peaks, beyond what is found in Bell03 and Withers12, see Mosenfelder et al. (2011) and Withers et al. (2011).
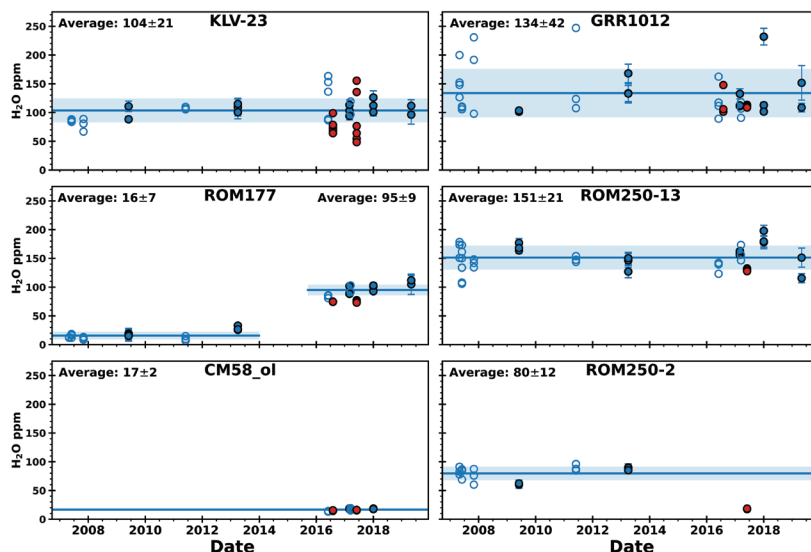
**FIGURE S4.** Concentrations of H_2O in olivine standards as determined from the same orthopyroxene calibration (India Enstatite, KBH-1, and ROM273) from 13 Carnegie SIMS sessions from 2007 to 2019. Blue symbols are data from the Cameca 6f ionprobe; red from the Nano-SIMS. Due to the limitations of the archived data most points do not have uncertainties (open circles); closed symbols include uncertainties. Concentrations given here are for the 6f ionprobe measurements only, and using the Bell et al. (1995) orthopyroxene calibration (they may be converted to the revised orthopyroxene calibration suggested in the text and Table 1 by multiplying by a factor of 0.93). For most samples, the precision within a single session is similar to the standard deviation of all sessions, suggesting that the variability is a feature of the samples and not due to changes in the orthopyroxene calibration. The measurements of the Bell03 NRA standards (KLV-23 and GRR1012) are highly variable due to the aforementioned hydrous non-olivine inclusions. We have omitted one measurement of KLV-23 because it plots ~10x higher than the other measurements. For the more homogeneous olivines, the standard deviation (1 sigma) is 12–14% over all sessions. ROM177 and ROM250-2 measurements include extremely low outliers that may have been on the wrong samples or that may reflect greater inter-specimen variability than previously recognized. The measurements of ROM177 after 2014 are consistent with the concentration measured by Bell et al. (2004) and Mosenfelder et al. (2011).
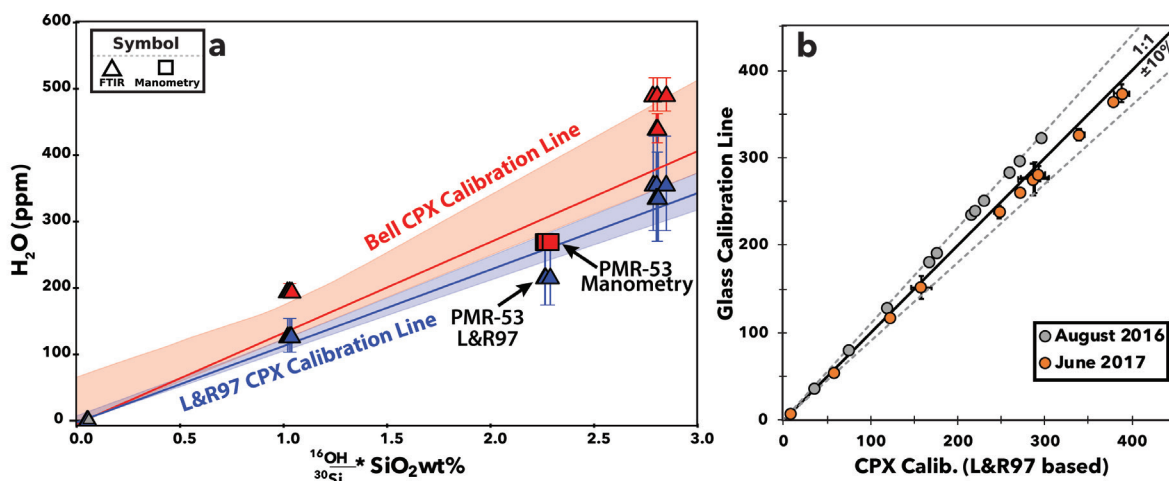
FIGURE S5. (**a**) Calibration lines for H$_2$O in clinopyroxene standards from Bell et al. (1995) and Bell et al. (2004). Ion counts (SiO$_2$ normalized) measured on the Carnegie NanoSIMS 50L (June 2017 session) are plotted vs. published values in Bell et al. (2004) and Mosenfelder and Rossman (2013b). The red points include the manometry value for PMR-53 (Bell et al. 1995) and FTIR determinations for the others, using the molar absorptivity from Bell et al. (1995). The blue points use the wavenumber-specific molar absorptivity in L&R97 (Libowitsky and Rossman, 1997), which leads to a marked improvement in the quality of the calibration, as noted by Mosenfelder and Rossman (2013b). We assumed a 20% uncertainty for the L&R97-based measurements. Methods for fitting lines and determining error envelopes (95%) are as is in Figure 1. All calibration lines are fit through a blank of Suprasil glass. (**b**) Concentrations measured in the clinopyroxene standards of Kumamoto et al. (2017) in two NanoSIMS sessions at Carnegie (different colored points) and using two different calibrations: L&R97 clinopyroxene (blue line in **a**) and basaltic glasses (y-axis). A one-to-one line with +/– 10% shows the excellent agreement between the two independent calibrations. Both calibrations return concentrations for PMR-53 within 5% of the manometry value.
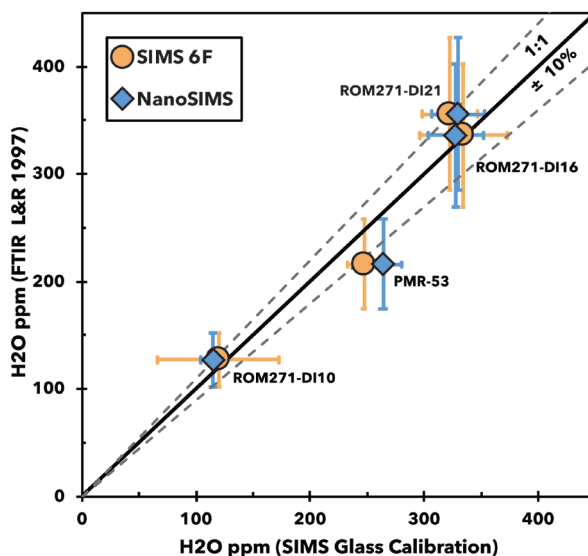
FIGURE S6. Comparison of FTIR and SIMS measurements for clinopyroxene standards from Bell et al. (1995) and Bell et al. (2004). The FTIR determinations were published by Mosenfelder and Rossman (2013b) and use the wavenumber dependent calibration in Libowitsky and Rossman (1997). Both SIMS and NanoSIMS determinations are calibrated using basaltic glasses. SIMS measurements are averaged from 9 sessions between 2007 and 2019 on the Carnegie Cameca 6F SIMS. NanoSIMS measurements are averages from the August 2016 and June 2017 sessions on the Carnegie NanoSIMS 50L. The black line is the 1:1 correlation line, showing excellent agreement generally within 10%. This supports the lack of a strong matrix effect between basaltic glasses and clinopyroxene measured by ion microprobe. The H$_2$O concentration for the clinopyroxene PMR-53 (calibrated using the basaltic glasses) averages 264±16 ppm on the NanoSIMS and 247±16 ppm on the 6F SIMS. These values agree well with the manometry value of 268 ±7.5 from Bell et al (1995), upon which Bell's molar absorptivity relies. The SIMS measurements of PMR-53, however, are offset from the other clinopyroxenes measured by FTIR using the Bell et al. (1995) molar absorptivity (Fig. S5a). This is well documented by Mosenfelder and Rossman (2013b), who find a wavenumber dependent calibration is necessary to rectify the offset and produce a linear SIMS calibration line.
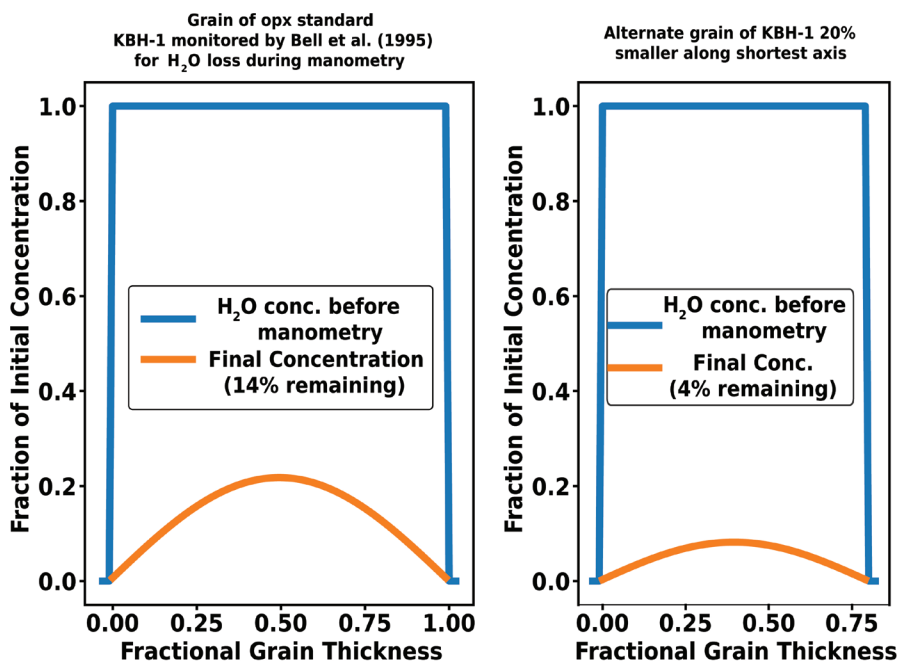
FIGURE S7. Finite difference diffusion models for hypothetical H$_2$O extraction in grains of orthopyroxene (KBH-1) during the manometry measurements of Bell et al. (1995). Diffusion is modeled in 1-dimension along the shortest axis of each grain. Diffusivities are assumed to be the same along this axis in both grains, a simplification made to demonstrate the effect of grain size alone on the fraction of H$_2$O extracted. The actual distribution of grain sizes and their respective crystallographic orientations is unknown but Bell et al. (1995) note that the grain they used to monitor H$_2$O loss before and after heating was one of the largest in the population. The x-axis of the plots is in fractional thickness relative to this grain. The y-axis is the fraction of H$_2$O in the crystal grains relative the initial conditions prior to manometry. The boundary condition at the grain edges is zero. The final concentrations (orange lines) are integrated to determine the total concentration remaining after the heating. This solution is independent of the diffusivity and time because both models use the same parameters, except for respective size, and are stopped at the time when the amount of remaining H$_2$O in the left-hand grain matches the amount measured by Bell et al. (1995): 14% of the initial concentration of H$_2$O. These hypothetical models are useful in conceptualizing how much H$_2$O might have been extracted from the whole population of KBH-1 grains heated during manometry. Given that the measured grain was notably larger than other grains, Bell et al. (1995) likely over corrected for unextracted H$_2$O in KBH-1, a point they also make when applying the 14% correction.
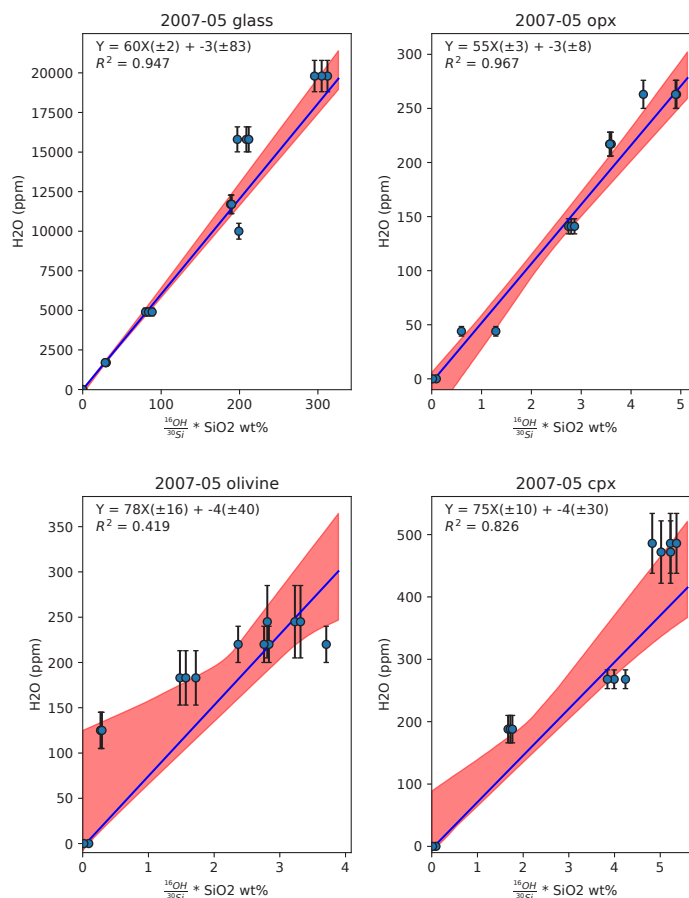
FIGURE S8. Compilation of H$_2$O calibration lines (2007 – 2019) fit to Cameca-6F SIMS measurements of Carnegie SIMS reference standards for glass, orthopyroxene, olivine, clinopyroxene. Linear regressions for these calibrations were fitted with the same weighted-orthogonal regression procedure as detailed in the Figure S1. Blue lines are the best fit linear calibrations for the measured standards. Red bands correspond to 95% confidence intervals for the calibration lines. Reference concentrations for clinopyroxene standards are consistent with the Bell et al. (1995) and Bell et al. (2004) values and not with the revised concentrations proposed in the text.

2007-11 glass

Y = 58X(±2) + -4(±62)
R^2 = 0.976

2007-11 opx

Y = 52X(±2) + -3(±3)
R^2 = 0.989

2007-11 olivine

Y = 72X(±20) + -4(±40)
R^2 = 0.055

2007-11 cpx

Y = 69X(±9) + -5(±22)
R^2 = 0.8

2009-06 glass
Y = 77X(±2) + -5(±49)
R^2 = 0.972

2009-06 opx
Y = 68X(±2) + -3(±5)
R^2 = 0.992

2009-06 olivine
Y = 128X(±39) + -7(±58)
R^2 = -0.042

2009-06 cpx
Y = 96X(±23) + -5(±59)
R^2 = 0.711

2011-06 glass

Y = 72X(±2) + -4(±0)
R^2 = 0.982

2011-06 opx

Y = 66X(±1) + -4(±0)
R^2 = 0.997

2011-06 olivine

Y = 87X(±13) + -5(±1)
R^2 = 0.643

2011-06 cpx

Y = 88X(±7) + -5(±1)
R^2 = 0.888

2017-03 glass
Y = 82X(±1) + 0(±0)
R^2 = 0.998

2017-03 opx
Y = 82X(±7) + 0(±0)
R^2 = 0.999

2017-03 olivine
Y = 117X(±6) + -1(±0)
R^2 = 0.951

2017-03 glass
$Y = 64X(\pm1) + -1(\pm0)$
$R^2 = 0.998$

2017-03 opx
$Y = 66X(\pm7) + -1(\pm0)$
$R^2 = 0.999$

2017-03 olivine
$Y = 97X(\pm6) + -2(\pm0)$
$R^2 = 0.939$

2018-01 glass

Y = 67X(±2) + 0(±0)
R^2 = 0.994

2018-01 opx

Y = 57X(±1) + 0(±0)
R^2 = 0.994

2018-01 olivine

Y = 71X(±5) + 0(±0)
R^2 = 0.899

2018-01 cpx

Y = 89X(±6) + -1(±1)
R^2 = 0.957